AIP Advances

Mini-stop bands in single heterojunction photonic crystal waveguides

N. Shahid, M. Amin, S. Naureen, and S. Anand

Citation: AIP Advances **3**, 032136 (2013); doi: 10.1063/1.4798304
View online: http://dx.doi.org/10.1063/1.4798304
View Table of Contents: http://scitation.aip.org/content/aip/journal/adva/3/3?ver=pdfcov
Published by the AIP Publishing

AIP ADVANCES **3**, 032136 (2013)

Mini-stop bands in single heterojunction photonic crystal waveguides

N. Shahid,[a] M. Amin,[b] S. Naureen, and S. Anand[c]
School of Information and Communication Technology, KTH- Royal Institute of Technology, Electrum 229, 164 40 Kista, Sweden

(Received 23 October 2012; accepted 7 March 2013; published online 20 March 2013)

Spectral characteristics of mini-stop bands (MSB) in line-defect photonic crystal (PhC) waveguides and in heterostructure PhC waveguides having one abrupt interface are investigated. Tunability of the MSB position by air-fill factor heterostructure PhC waveguides is utilized to demonstrate different filter functions, at optical communication wavelengths, ranging from resonance-like to wide band pass filters with high transmission. The narrowest filter realized has a resonance-like transmission peak with a full width at half maximum of 3.4 nm. These devices could be attractive for coarse wavelength selection (pass and drop) and for sensing applications. [http://dx.doi.org/10.1063/1.4798304]

Two dimensional (2D) photonic crystals (PhCs) have fostered a rapidly growing interest and several novel phenomena and applications such as strong light confinement, slow light, spatial dispersion, and filtering have been demonstrated.[1] Engineering defects in the otherwise periodic structure has been very effectively used for waveguides[2] and small mode volume high Q cavities.[3] The availability of optical sources at telecom wavelengths in InP based materials has made them attractive for PhC devices and both high-index contrast structures (membrane type) and low-index contrast structures (substrate-type) have been extensively investigated. The substrate-type InP-based PhCs are attractive due to their compatibility for integration with conventional photonic components on InP substrate. Several PhC devices in the substrate approach such as demultiplexer,[4] laser[5] and filters[6] have been demonstrated and this has been possible due to the development of deep etching of PhCs in InP.[7,8]

PhC waveguides have received much attention for their unique slow light[9] and dispersion control[10,11] properties. Recently a new class of photonic crystal components/structures has emerged, namely photonic crystal heterostructures.[12] Similar to semiconductor heterostructures, photonic heterostructures are composed of two photonic crystals with different band-gaps obtained either by changing the air-fill factor (f),[13,14] or by the lattice constant (a). New functions such as high Q cavities,[15] electro-optic modulator[16] and fluid sensors[17] have been experimentally demonstrated using the concept of heterostructures. These categories of devices essentially use double-heterostructures. Cascading of heterostructures towards a PhC superlattice has also been demonstrated for the conservation of phase despite the change in the physical path length.[18] Juxtaposing PhC in a beam-splitter configuration has been demonstrated for polarization beam splitter.[19,20] The use of single-junction heterostructures for low-loss waveguide bends has been theoretically investigated.[21] Hitherto, there are no reports on heterostructure PhC waveguides in deeply etched PhCs. In particular, the multi-mode line defect waveguides with "internal" mini-stop band (MSB)

[a]Present address: Australian National Fabrication Facility - ACT Node, Department of Electronic Materials Engineering, Research School of Physics and Engineering, The Australian National University, Canberra ACT 0200, Australia
[b]Present address: Division of Physical Sciences and Engineering, King Abdullah University of Science and Technology, Thuwal, 23955-6900, Saudi Arabia.
[c]Author to whom correspondence should be addressed. Electronic mail: anand@kth.se

effect[22,23] due to mode-coupling could bring a new dimension both for fundamental physics and applications. MSBs in heterostructure waveguides could have interesting applications such as designable band-pass flat-top filters, and resonance-like filters with high transmission. Here, we note that the technology of deeply etched PhCs in InP has been improved only recently to obtain nearly cylindrical hole-shapes.[24,25] Using this improved process, it has been possible to realize line-defect waveguides with superior MSB characteristics in terms of sharpness of transmission band-edges and attenuation,[24,26,27] and of propagation loss in single-row defect waveguides.[23]

In this letter, we experimentally demonstrate planar filters in transmission geometry that utilize the internal mode-gap concept in single junction heterostructure PhC waveguides (three row missing-W3). The single junction heterostructure PhC waveguides (HPCW) are realized as a two-segment W3 waveguide with different air-fill factors but with the same period. A 60 nm wavelength shift in the position of MSB in 60 row long W3 waveguides for 18% change in the fabricated *f* is experimentally demonstrated. In a 120 row HPCW (with a single interface), by appropriate choice of air-fill factors we demonstrate different filter shapes ranging from resonance-like to wide band pass filters with high transmission. In the MSB regions, the attenuation is as high as 25 dB for a 60 row ($\sim 25\ \mu$m) long waveguide.

We used PhC waveguides created by removing three rows in the ΓK direction from a triangular lattice of air-holes, typically referred to as a W3 PhC waveguide,[22] which exhibits a MSB in transmission for the fundamental mode. We consider an InP/InGaAsP/InP heterostucture (with refractive indices n = 3.17 (InP) and 3.35 (InGaAsP)). The upper InP cladding is 300 nm thick and InGaAsP core is 520 nm. For this vertical structure the effective index is $n_{eff} = 3.2$. In W3 waveguides coupling of modes with the same symmetry is known to result in mode-gaps or mini-gaps.[23–26] In this work, we focus on the mode-gap arising from coupling between the fundamental mode (0^{th} order) and the fourth order mode. Figure 1(a) shows this mode coupling region in the dispersion diagrams of W3 waveguides with different air-fill factors calculated by plane-wave expansion (PWE) method. The PWE calculations were made for TE polarization for *f* ranging from 30 to 55%. Also shown are the mode profiles of the fundamental and the fourth order modes (Fig. 1(b) and 1(c), respectively) obtained sufficiently far away from the mode-gap. As shown on Fig. 1(a), for the W3 waveguide with $f = 30\%$ the mode-gap occurs around $u = 0.265$; where $u = a/\lambda$ is normalized frequency, *a* is the lattice period and λ the wavelength. As *f* increases, the position of the mode-gap shifts to higher frequencies [Fig. 1(a)]. As a consequence, transmission MSB in such waveguides will also follow this trend with air-fill factor. Thus if two W3 waveguides having different air-fill factors are put together as a HPCW, it is possible to obtain different filter functions by designing the spectral position and the overlap of the MSBs in the two waveguides.

In order to correlate optical fill factors with MSB positions, transmission spectra were simulated by the finite-difference time-domain (FDTD) method. We use a 2D FDTD method with Perfect Matched Layer (PML) boundary treatment for numerical simulation. The shift in MSB central frequency as function of *f* is shown by dashed line on Fig. 2. The MSB shifts nearly linearly towards higher frequencies inside photonic band-gap. A frequency shift of $\Delta u = 4.5 \times 10^{-3}$ is determined for 20% change in *f*. For a lattice constant of 420 nm it corresponds to 79 nm shift in the wavelength of operation. The cross marks on Fig. 2 indicate the experimentally determined MSB central positions and the corresponding *f* determined by high resolution SEM (top-view) analysis of the fabricated devices. The MSB positions obtained in the experiments with respect to fabricated *f* are in good agreement with the calculations performed by PWE and FDTD. Thus, the data of Fig. 2 shows that HPCWs can be fabricated with appropriate choice of *f* to investigate different filter functions.

The InP/InGaAsP/InP low index contrast slab was grown by metal organic vapor phase epitaxy (MOVPE) on InP substrate. The InP cap and the GaInAsP core lattice matched to InP ($\lambda_{gap} = 1.22\ \mu$m) were 300 nm and 520 nm thick, respectively. The PhC waveguide oriented in the Γ-K direction consists of three missing rows in a triangular lattice of air-holes with a period of 420 nm, and is 120 row long. The PhC patterns were made by electron beam lithography using ZEP520 as the resist. The patterns were then transferred in to a 260 nm thick SiO_2 mask using CHF_3 based reactive ion etching. Subsequently the PhCs were etched using Ar/Cl_2 chemically assisted ion beam etching (CAIBE). Details of the etching process and process conditions are given in Ref. 28. The fabricated HPCWs are 120 rows long having an abrupt interface between the two segments with

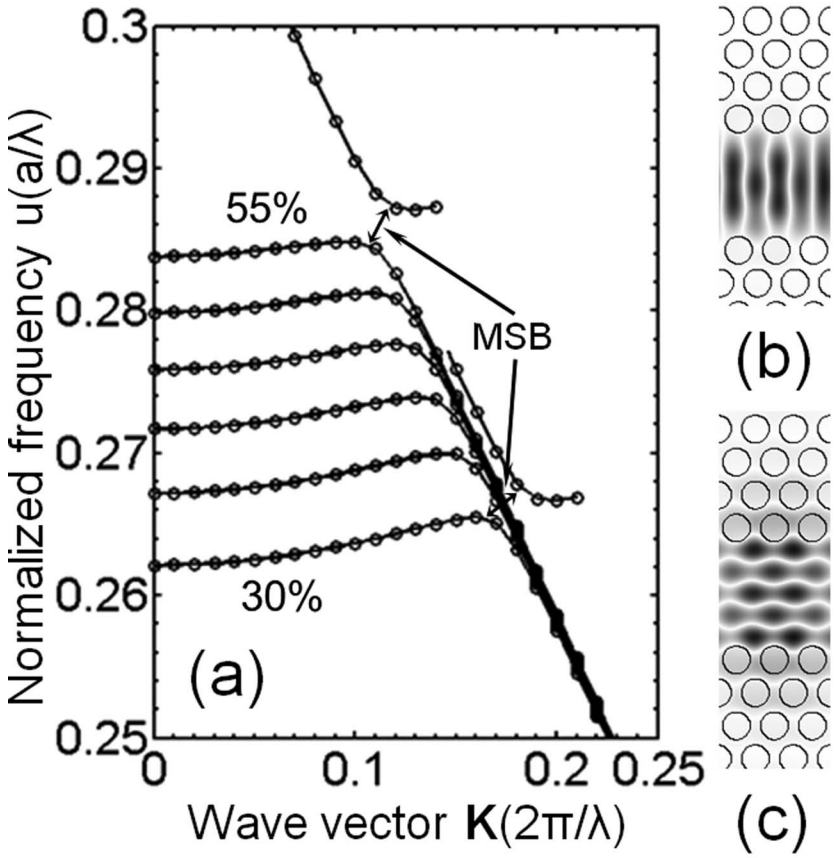

FIG. 1. (a) Dispersion diagram of the W3 Waveguide showing the investigated mode-gap and its evolution with *f* which was varied from 30 to 55%. Mode profiles of (b) 0^{th} order mode and (c) 4^{th} order mode sufficiently far away from the mode-gap region.

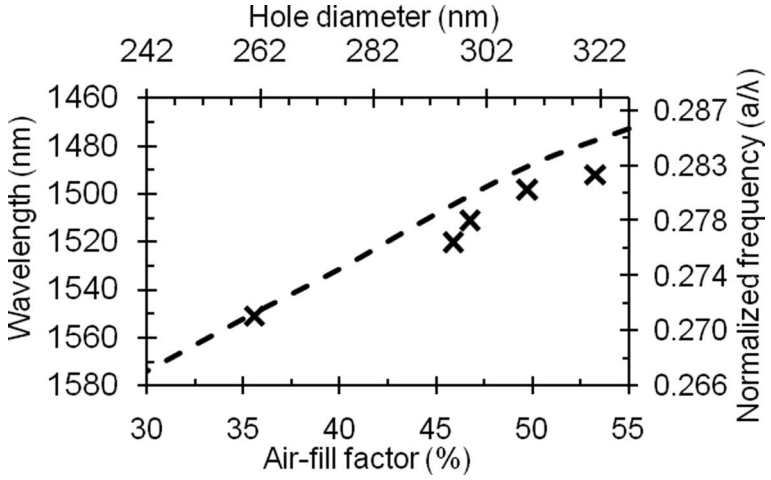

FIG. 2. MSB central frequency vs. *f* for W3 PhC waveguide. Secondary axes are scaled with a lattice constant a = 420 nm. The dashed line represents MSB shift obtained by 2D FDTD calculations while the "X" symbols the experimental determined air fill factors central MSB positions.

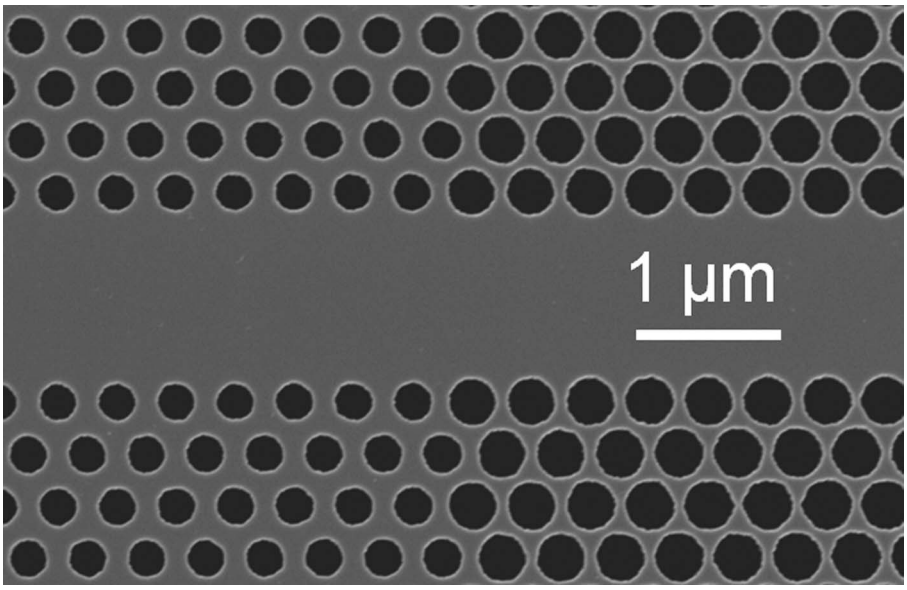

FIG. 3. HPCW showing the junction region; the change in the air-fill factor (same period) is clearly visible. The change in f between the two sections is $\Delta f = 13\%$ (designed value).

having different f, each 60 row long. The designed air-fill factor difference (Δf) between the two sections was 3%, 5% and 13%. Figure 3 shows a SEM image at the junction of a typical fabricated HPCW having the largest Δf; the difference in hole-diameter in the two sections is clearly visible.

The PhC waveguides were characterized by the standard end-fire characterization technique. A tunable laser source having a spectral range 1460–1580 nm was used as the light source, and was coupled into the cleaved facet of the input access ridge waveguide through a focusing gradient index lens. The output light is collected by a microscope objective and split into two beams, one to an infrared camera for alignment and imaging, and, the other to an optical spectrum analyzer through a single mode fiber to measure the transmission spectra. TE polarizers were used at both input and output of the sample.

Figure 4 shows the measured transmission spectra for the HPCW where the characteristic dips in transmission due to the MSB effect are visible. The location of the MSB inside photonic band-gap depends on f (Fig. 2) and moves towards shorter wavelengths (or higher u) as f increases. Figure 4(a) demonstrates a flat transmission level for a broadband between two MSBs with 3 dB bandwidth 65 nm. Only a part of the MSB for highest f is visible due to the limited wavelength range of the tunable laser used in the experiment. The designed $\Delta f = 13\%$ was the largest which is clearly distinguishable in Fig. 3. A slightly lower level of peak transmission in case of HPCW with $\Delta f = 5\%$ (Fig. 4(b)) is due to the overlap of two MSB cut off at slightly lower transmission level (compared to one outside MSB). Such in plane pass filters can be attractive for course wavelength selection from a broadband source. The MSB band-edges in HPCWs behave in the same manner as in single W3 waveguide. A resonance–like peak with FWHM 3.4 nm is obtained between two stop-bands by having $\Delta f = 3\%$ (Fig. 4(c)). This HPCW shows a sufficiently sharp transmission peak where the detection of peak wavelength is straightforward and could potentially be interesting for sensing applications. The transmission level and the sharpness of the peak are related to the obtained sharpness of the MSB edges[24,26] in the respective section of the waveguide. Finally, as expected for linear systems the measured characteristics (Fig. 4) do not change with reversing the order of the two sections.

Recently, we demonstrated wavelength tuning of MSB by varying the waveguide width.[27] Juxtaposing two waveguides with slightly different widths, but having the same air-fill factor and period, a pass-filter function was obtained. The approach used in the present work is different, and is based on air-fill factor tuning of the MSB position. Both approaches are equally viable to achieve the different filter functions shown on Fig. 4, and the width of the MSB (notch) can also be increased

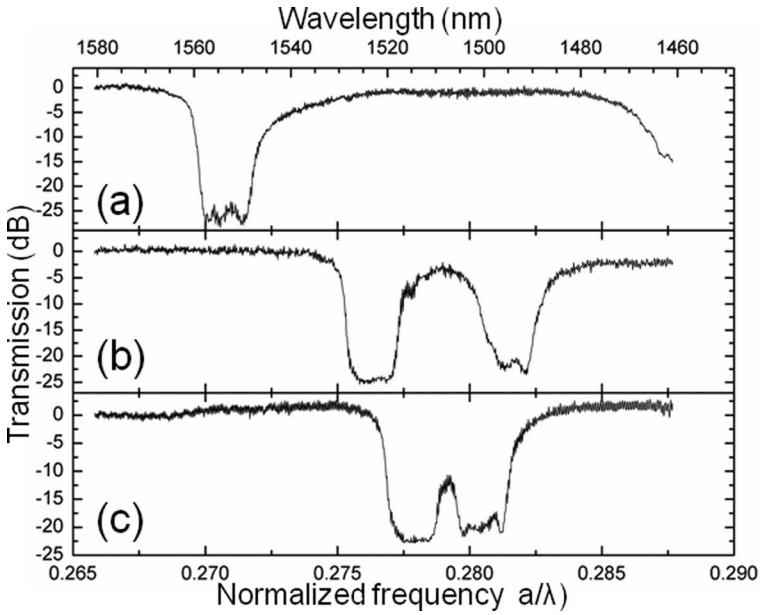

FIG. 4. Measured Transmission spectra (normalized) for HPCWs for designed (a) $\Delta f = 13\%$ (b) $\Delta f = 5\%$ and (c) $\Delta f = 3\%$.

by appropriately cascading the waveguides. However, the two approaches can be compared in terms of the obtained results and device fabrication accuracy. For a fixed period (420 nm) the measured wavelength tuning range of the MSB position was about 130 nm by changing the waveguide width.[27] In comparison, variation of the air-fill factor within a reasonable values (~30 to 55%) yielded a lower value of 79 nm wavelength tuning range for the MSB. Although resonance-like filters have been realized by both approaches (here, for example Fig. 4(c)), the results obtained using the wave-guide width approach demonstrates superior transmission characteristics with only 5 dB attenuation of the transmission peak.[27] Although the present results are better in terms of the line-width of the resonance-like filter, i.e, 3.4 nm compared to 5.6 nm reported in ref. 27, it has comparatively poor transmission. From a technology point of view, the main difficulty arises in controlling the air-fill factor while writing the pattern and in the subsequent pattern transfer steps. Even if the air-fill factor can be well controlled, it would be necessary to modify the dispersion of the modes near the coupling region to achieve band-widths and edges of the notch or pass filters narrower and sharper than those shown on Fig. 4. Another possibility is to study the variation of the MSB shape and position with period, keeping the air-fill factor and waveguide width fixed. This will provide yet another way to obtain the different filter shapes shown in Fig. 4. Irrespective of the approaches, realization of MSB with tailored transmission edges is necessary to realize desired pass-filter shapes, e.g. Gaussian or box-like. We believe that a combination of all the three parameters - air-fill factor, waveguide width and period –to engineer the waveguide around the junction may be necessary to improve the filter characteristics.

In conclusion, we have implemented the tune-ability of MSB with respect to the f in a W3 PhC waveguide. A 60 nm shift in the position of MSB for 18% change in fabricated f was experimentally demonstrated. A correlation between MSB (shape and position) and f is established which emphasize nanoscale precision in the fabrication of 2D PhCs. In a 120 row long HW3 PhC waveguide, by appropriate choice of the air-fill factor we could obtain different filter shapes ranging from resonance-like to wide band pass filters with high transmission. The sensitivity for refractive index changes of the high transmission sharp peak realized by overlapping two MSBs could be attractive towards sensing, tuning and modulation applications. By fine-tuning the junction interface, for example by band-gap grading, optical properties can be further engineered.

ACKNOWLEDGMENTS

Support from the Swedish Research Council (VR) is gratefully acknowledged. The work was performed within the Linné Center in Advanced Optics and Photonics (ADOPT). N. Shahid and S. Naureen acknowledge Higher Education Commission, Pakistan for partially supporting their PhD studies. The authors thank M. Swillo for useful discussions.

[1] M. Notomi, Rep. Prog. Phys. **73**, 096501 (2010).
[2] L. Thylén, M. Qui, and S. Anand, ChemPhysChem. **5**, 1268 (2004).
[3] E. Kuramochi, M. Notomi, S. Mitsugi, A. Shinya, T. Tanabe, and T. Watanabe, Appl. Phys. Lett. **88**, 041112 (2006).
[4] M. Ayre, C. Cambournac, O. Khayam, H. Benisty, T. Stomeo, and T. F. Krauss, Photonics and Nanostructures, Fundamentals and Applications **6**, 19–25 (2008).
[5] S. A. Moore, L. O'Faolain, T. P. White, and T. F. Krauss, Opt. Express **16**, 1365 (2008).
[6] M. Devanco, A. Xing, J. W. Raring, E. L. Hu, and D. J. Blumenthal, IEEE J. Selected Topics in Quantum Electronics **12**, 1164 (2006).
[7] M. Mulot, S. Anand, M. Swillo, M. Qiu, B. Jaskorzynska, and A. Talneau, J. Vac. Sci. Technol. B **21**, 900 (2003).
[8] M. V. Kotlyar, T. Karle, M. D. Settle, L. O'Faolain, and T. F. Krauss, Appl. Phys. Lett. **84**(18), 3588 (2004).
[9] T. Baba, Nat. Photon. **2**(8), 465–473 (2008).
[10] M. Notomi, K. Yamada, A. Shinya, J. Takahashi, C. Takahashi, and I. Yokohama, Phys. Rev. Lett. **87**, 253902 (2001).
[11] A. D. Falco, L O'Faolain, and T. F. Krauss, Appl. Phys. Lett. **92**, 083501 (2008).
[12] E. Istrate and E. H. Sargent, Rev. Mod. Phys. **78**, 455 (2006).
[13] S-H. Koon, T. Sünner, M. Kamp, and A. Forchel, Opt. Express **16**, 4605 (2008).
[14] S-H. Koon, T. Sünner, M. Kamp, and A. Forchel, Opt. Express **16**, 11709 (2008).
[15] B.-S. Song, S. Noda, T. Asano, and Y. Akahane, Nat. Mat. **4**(3), 207–210 (2005).
[16] J. H. Wülbern, J. Hampe, A. Petrov, M. Eich, J. Luo, A. K. -Y. Jen, A. D. Falco, T. F. Krauss, and J. Bruns, Appl. Phys. Lett. **94**, 241107 (2009).
[17] A. D. Falco, L. O'Faolain, and T. F. Krauss, Appl. Phys. Lett. **94**, 063503 (2009).
[18] S. Kocaman, M. S. Aras, D. L. Kwong, A. Stein, P. Hsieh, C. W. Wong, J. F. McMillan, C. G. Biris, N. C. Panoiu, M. B. Yu, D. L. Kwong, A. Stein, and C. W. Wong, Nat. Photon. **5**, 499–505 (2011).
[19] E. Schonbrun, Q. Wu, W. Park, T. Yamashita, and C. J. Summers, Opt. Lett. **31**(21), 3104 (2006).
[20] Y. Shi, N. Shahid, M. Li, A. Berrier, S. He, and S. Anand, Optical Engineering **49**(6), 060503 (2010).
[21] H. Kurt and D. S. Citrin, IEEE J Quantum Electron. **43**(1), 78 (2007).
[22] C. J. M. Smith, H. Benisty, S. Olivier, M. Rattier, C. Weisbuch, T. F. Krauss, R. M. De la Rue, R. Houdre, and U. Oesterle, Appl. Phys. Lett. **77**, 2813–2815 (2000).
[23] S. Olivier, M. Rattier, H. Benisty, C. Weisbuch, C. J. M. Smith, R. M. De La Rue, T. F. Krauss, U. Oesterle, and R. Houdré, Phys. Rev. B **63**, 113311 (2001).
[24] N. Shahid, S. Naureen, M. Y. Li, M. Swillo, and S. Anand, J. Vac. Sci. Technol. B **29**, 031202 (2011).
[25] R. Kappeler, P. Kaspar, H. Jäckel, and Ch. Hafner, Appl. Phys. Lett. **101**, 131108 (2012).
[26] N. Shahid, N. Speijcken, S. Naureen, M. Y. Li, M. Swillo, and S. Anand, Appl. Phys. Lett. **98**, 0811121 (2011).
[27] N. Shahid, M. Amin, S. Naureen, M. Swillo, and S. Anand, Opt. Express **19**(21), 21074 (2011).
[28] A. Berrier, M. Mulot, A. Talneau, R. Ferrini, R. Houdré, and S. Anand, J. Vac. Sci. Technol. B **25**, 1 (2007).